Published in final edited form as:
Mucosal Immunol. 2011 September ; 4(5): 503–518. doi:10.1038/mi.2011.16.

Free Radical-Producing Myeloid-Derived Regulatory Cells: Potent Activators and Suppressors of Lung Inflammation and Airway Hyperresponsiveness

Jessy Deshane[1,2,5], **Jaroslaw W. Zmijewski**[2,5], **Rita Luther**[1], **Amit Gaggar**[2,8], **Rohit Deshane**[1], **Jen-Feng Lai**[1], **Xin Xu**[2], **Marion Spell**[2,6], **Kim Estell**[3], **Casey T Weaver**[4], **Edward Abraham**[2,5], **Lisa M. Schwiebert**[3,5], and **David D. Chaplin**[1,5,7]

[1]Department of Microbiology, University of Alabama at Birmingham, Birmingham, Alabama 35294

[2]Department of Medicine, University of Alabama at Birmingham, Birmingham, Alabama 35294

[3]Department of Physiology and Biophysics, University of Alabama at Birmingham, Birmingham, Alabama 35294

[4]Department of Pathology, University of Alabama at Birmingham, Birmingham, Alabama 35294

[5]Center for Free Radical Biology, University of Alabama at Birmingham, Birmingham, Alabama 35294

[6]Center for AIDS Research, University of Alabama at Birmingham, Birmingham, Alabama 35294

[7]Arthritis and Musculoskeletal Center, University of Alabama at Birmingham, Birmingham, Alabama 35294

[8]Veteran Affairs Medical Center, University of Alabama at Birmingham, Birmingham, Alabama 35294

Abstract

Levels of reactive free radicals are elevated in the airway during asthmatic exacerbations, but their roles in the pathophysiology of asthma remain unclear. We have identified subsets of myeloid-derived suppressor-like cells as key sources of nitric oxide and superoxide in the lungs of mice with evolving experimental allergic airway inflammation and established these cells as master regulators of the airway inflammatory response. The profiles of free radicals they produced depended on expression of iNOS, arginase, and NADPH oxidase. These radicals controlled the pro- and anti-inflammatory potential of these cells, and also regulated the reciprocal pattern of their infiltration into the lung. The nitric oxide-producing cells were Ly-6C+Ly-6G$^-$ and down-modulated T cell activation, recruited T_{reg} cells, and dramatically down-regulated antigen-induced airway hyperresponsiveness. The superoxide-producing cells were Ly-6C$^-$Ly-6G$^+$ and expressed proinflammatory activities, exacerbating airway hyperresponsiveness in a superoxide-dependent fashion. A smaller population of Ly-6C$^+$Ly-6G$^+$ cells also suppressed T cell responses, but in an iNOS- and arginase-independent fashion. These regulatory myeloid cells represent important targets for asthma therapy.

Address for correspondence: David D Chaplin M.D, Ph.D., Department of Microbiology, University of Alabama at Birmingham, 845 19th Street South, Birmingham, AL 35294. Tel: (205)-934-9339, Fax:(205)-934-9256, dchaplin@uab.edu.

DISCLOSURE. All of the authors assert that they have no conflicts of interest relevant to the work described in this manuscript.

INTRODUCTION

Asthma is a disorder of respiratory function characterized by persistent Th2-predominant inflammation and reversible airway obstruction, associated with airway hyperresponsiveness (AHR).[1] Studies in experimental models of asthma indicate that both innate and adaptive immune cells contribute to asthma pathogenesis.[2, 3] Although lymphoid and myeloid cell-derived cytokines and chemokines are recognized to contribute to the asthmatic phenotype, the mediators that induce AHR remain incompletely defined.[2, 3] Reactive free radicals such as nitric oxide (NO) and superoxide ($O_2^{\cdot -}$), which can either augment or suppress inflammatory processes, have been identified in the airways of asthmatic subjects;[4-7] however, the cellular sources of these molecules and their relationship to the major features of the asthmatic phenotype remain unknown.

The bioavailability of NO is regulated *in vivo* at the level of its production from L-arginine (L-Arg) by nitric oxide synthases (NOS), particularly the inducible NOS (iNOS), and its consumption in downstream chemical reactions.[8-10] The ability of eosinophil cationic proteins to inhibit the transport and availability of L-Arg, thereby reducing the production of bronchodilatory NO in the airway, has been implicated in the induction of AHR;[11] however, increased levels of NO in exhaled breath condensate and bronchoalveolar lavage (BAL) fluid from asthmatics[5, 12] suggest that NO can have pro-inflammatory effects. Peroxynitrite ($ONOO^-$), generated by reaction of NO and $O_2^{\cdot -}$, is also a biomarker of airway inflammation.[7, 13] Studies with inhibitors of NO and $O_2^{\cdot -}$ also highlight NO and $O_2^{\cdot -}$ as drivers of AHR in asthma.[14, 15] NO, with its dual potential, supporting physiological functions and tissue homeostasis as well as activating inflammation, has remained a paradox in the context of asthmatic inflammation.

Pharmacological inhibition of arginase has also been reported both to improve and to worsen inflammation in experimental asthma.[10, 16, 17] Arginase catalyzes the conversion of L-Arg to urea and polyamines, which can contribute to airway remodeling in chronic asthma.[10, 17] Activation of arginase depletes L-Arg, not only reducing bioavailable NO because of limitations of substrate[10, 17] but also uncoupling the NOS enzymes leading to increased production of $O_2^{\cdot -}$.[18] Thus, competition between arginase and iNOS for L-Arg can upset the important NO/$O_2^{\cdot -}$ balance in asthmatic lungs.[17] Regulated expression of NADPH oxidase also controls $O_2^{\cdot -}$ production in the local tissue environment.[19]

Populations of immature myeloid cells called Myeloid-Derived Suppressor Cells (MDSC) can produce free radicals using the iNOS, arginase and NADPH oxidase pathways.[20, 21] MDSC, broadly characterized in mice by their surface expression of the Gr-1 and CD11b antigens, are immunosuppressive in cancer,[20, 22] autoimmune and viral encephalitis[23], inflammatory bowel disease[24], and other conditions[25-27] where they inhibit both CD4 and CD8 T-cell proliferative responses via their production of NO and $O_2^{\cdot -}$[28]. Their free radical products also contribute to the recruitment, maintenance, and activation of the MDSC themselves.[20, 21] The participation of MDSC in determining the balance of the iNOS, arginase, and the NADPH oxidase pathways in a Th2 cell-dominant inflammatory disorder like asthma is undefined. We hypothesized that asthmatic inflammation and AHR are regulated by mechanisms that involve accumulation of free radical-producing MDSC-like cells in lungs.

In this study, we identify three populations of Gr-1^+CD$11b^+$ myeloid cells that infiltrate the lung in a mouse model of allergic airway inflammation where they differentially generate the reactive free radicals NO and $O_2^{\cdot -}$. The Ly-$6C^+$ Ly-$6G^-$ subset (predominant NO producer) and the Ly-$6C^+$Ly-$6G^+$ subset suppress T cell proliferation *in vitro*. The $O_2^{\cdot -}$-generating Ly-$6C^-$Ly-$6G^+$ subset, in contrast, enhances T cell responses. We refer to these

Gr-1$^+$CD11b$^+$ myeloid cells as Myeloid-Derived *Regulatory* Cells (MDRC) to acknowledge their potential either to suppress or to augment immune and inflammatory responses. Using pharmacological inhibitors and/or mouse strains with genetic knockout of the iNOS, arginase or NADPH oxidase pathways, we show an integral role for these enzymes and their metabolites in the accumulation of the MDRC in the lungs. Importantly, intratracheal (i.t.) adoptive transfer of MDRC subsets dramatically modulates AHR. Our studies thus highlight the functional significance of enzymes that produce free radicals and their metabolites in the induction and suppressive potential of the myeloid lineage in experimental allergic airway disease. Identifying MDRC as important sources of free radicals in the inflamed lung provides a new perspective on the role of NO in asthma.

Results

The iNOS and arginase pathways are induced in experimental asthma

This study was undertaken to test whether the iNOS, arginase and NADPH oxidase pathways participate in antigen-driven inflammatory responses of the airways and whether the free radical products of these pathways are central to these responses. We first examined the levels of the NO metabolite nitrite and the end product of the arginase pathway urea in BAL fluid of ovalbumin (OVA) sensitized and challenged mice. In the OVA challenged C57BL/6 (wild type; wt) mice, nitrite was increased in BAL fluid at d2, with a modest but significant reduction at d3 and a progressive rise from d5 to d10 (Figure 1a, cross-hatched bars). This increase in nitrite was not observed in OVA-challenged iNOS$^{-/-}$ mice (Figure 1a, open bars) suggesting that iNOS-derived NO is the source of nitrites in BAL fluid of asthmatic wt mice. Levels of urea were elevated in BAL fluid at d3 following i.n. OVA challenge (Figure 1b, cross-hatched bars), indicating that arginase activity was also increased in the antigen driven airway inflammatory response. The iNOS and arginase enzymes compete for the same substrate L-Arg and metabolites of the arginase pathway increase in the absence of functional iNOS.[29] Consistent with this, analysis of OVA sensitized and challenged iNOS$^{-/-}$ mice showed a significant elevation of the levels of urea in BAL fluid during the inflammatory response (Figure 1b, open bars), compared to wt animals, indicating that activation of the arginase pathway is enhanced in the absence of functional iNOS.

To identify the cell types that express iNOS and arginase in allergic airway responses, we analyzed leukocyte populations that accumulated in the lungs of OVA sensitized and challenged wt mice. The numbers of infiltrating leukocytes peaked at d3 after OVA challenge of wt mice (Figure 1c). The numbers of neutrophils (Gr-1$^+$CD11b$^+$F4/80$^-$) were highest at d2 and d3 after challenge (Supplementary Figure 1a), preceding the influx of Sca-1$^+$CD34$^+$CCR3$^+$ eosinophils (Supplementary Figure 1b). The numbers of CD3$^+$ T lymphocytes were also increased after antigen challenge consistent with other studies using the OVA sensitization and challenge protocol (data not shown). Cellular infiltrates, including neutrophils and eosinophils, were reduced in the iNOS$^{-/-}$ mice (Figure 1c, Supplementary Figures 1a and b). The Th1 cytokine IFN-γ and the Th2 cytokines IL-4, IL-5, and IL-13 and the Th2-associated factor GM-CSF were elevated in the BAL fluid from OVA challenged wt mice during this phase of the response. The relatively lower levels of Th2 cytokines (Supplementary Figure 1c) were consistent with the results of Gueders et al. who showed that the levels of Th2 cytokines are lower in BAL fluid collected from sensitized and challenged C57BL/6 mice compared to mice of the BALB/c strain.[30] Eotaxin levels were also increased in BAL fluid over a similar time course (Supplementary Figure 1d).

MDSC-like cells accumulate in the lungs during allergic inflammation

In inflammatory responses, myeloid lineage cells are known to be major producers of NO and other free radical species. Therefore, we next characterized the phenotype of myeloid lineage cells recovered from the lungs of antigen sensitized and challenged wt mice. At d2 after OVA challenge, 24% of the total infiltrating leukocytes were Gr-1^{+}CD11b^{+} cells (Figure 2a, **left panel**). Within this population, a subset of Gr-1^{hi}CD11b^{hi} cells represented 9% of the total lung leukocytes, with >90% of these being F4/80^{+} (Figure 2a, **middle panel**). Within the Gr-1^{+}CD11b^{+}F4/80^{+} population, we detected 3 distinct myeloid cell subsets, characterized as Ly-6C^{+}Ly-6G^{-}, Ly-6C^{-}Ly-6G^{+} and Ly-6C^{+}Ly-6G^{+}, (Figure 2a, **right panel**). The Ly-6C^{+}Ly-6G^{-} subset had lower CD11b expression compared to the Ly-6C^{-}Ly-6G^{+} and Ly-6C^{+}Ly-6G^{+} subsets within Gr-1^{hi} gated cells (data not shown). Analysis after purification by flow cytometric sorting (Figure 2b) indicated a monocytoid morphology for the Ly-6C^{+}Ly-6G^{-} subset (Figure 2c, left panel), macrophage morphology for the Ly-6C^{-}Ly-6G^{+} subset (Figure 2c, **center panel**), and granulocyte-like polymorphonuclear characteristics for the Ly-6C^{+}Ly-6G^{+} subset (Figure 2c, **right panel**). The monocytoid subset also expressed the MDSC-associated mCSF-1 receptor[31] (CD115; Supplementary Figure 2a). The macrophage mannose-receptor CD206, another MDSC-associated antigen, was expressed by CD11b^{+}Ly-6G^{+} cells (Supplementary Figure 2b). Thus, these cell subsets have phenotypic characteristics of MDSC.

Lung MDSC-like cells utilize iNOS, arginase and NADPH oxidase for production of free radicals

Cancer MDSC use the iNOS, arginase and NADPH oxidase pathways to generate free radicals necessary for their function.[20, 32] Ly-6C^{+}Ly-6G^{-} cells purified by fluorescence-activated cell sorting (FACS) from lungs of OVA sensitized and challenged wt mice, at both d2 and d5 after challenge, generated micromolar concentrations of NO (detected as nitrite) after *in vitro* culture for 48 h (Figure 3a, black bars **and** Supplementary Figure 3). Purified Ly-6C^{-}Ly-6G^{+} cells showed no increase in NO production (Figure 3a, gray bars **and** Supplementary Figure 3). Increased NO production by Ly-6C^{+}Ly-6G^{-} cells was dependent on expression of functional iNOS and NADPH oxidase, with no increase observed in cultures of Ly-6C^{+}Ly-6G^{-} cells from iNOS$^{-/-}$ mice and significantly higher levels of NO production in NADPH oxidase deficient Ly-6C^{+}Ly-6G^{-} cells (Figure 3a). 95% of the DAF-FM-DA^{+} cells from the total lung infiltrates in OVA challenged wt mice at d2 were Ly-6C^{+}Ly-6G^{-} **(**Supplementary Figure 4**)**. With the caveat that our digestion procedure may not liberate all lung stromal cells in viable form, these results confirm these MDSC-like cells as the predominant source of NO during airway inflammation, while epithelial cells, neutrophils, eosinophils and perhaps stromal cells together represent approximately 5% of the DAF-FM-DA^{+} cells. Ly-6C^{+}Ly-6G^{-} cells purified from wt mice at d5 after challenge (Figure 3b, blue tracing) stained positive with the fluorescent NO indicator dye DAF-FM-DA, while none of the wt Ly-6C^{-}Ly-6G^{+}, wt Ly-6C^{+}Ly-6G^{+} or iNOS$^{-/-}$ Ly-6C^{-}Ly-6G^{+} cells were DAF-FM-DA^{+}. The specificity of DAF-FM-DA for NO was demonstrated by the fact that incubation of wt Ly-6C^{+}Ly-6G^{-} cells with the specific iNOS inhibitor 1400w inhibited the staining with DAF-FM-DA (Figure 3b, green tracing).

Lung MDSC-like cells showed reciprocal patterns of expression of the products of the iNOS and arginase pathways. Ly-6C^{-}Ly-6G^{+} cells, which did not have the potential to produce NO when purified at d3 after challenge, produced higher levels of urea compared to the NO-producing Ly-6C^{+}Ly-6G^{-} subset (Figure 3c, gray bars and black bars, respectively). Interestingly, production of urea by iNOS$^{-/-}$ Ly-6C^{-}Ly-6G^{+} cells was higher compared to wt or p47 m cells (Figure 3c). These results are consistent with the elevated concentration of urea found in BAL fluid recovered from iNOS$^{-/-}$ mice at d3 (Figure 1b). In contrast, granulocytic Ly-6C^{+}Ly-6G^{+} cells produced modest levels of urea (Figure 3c, open bars).

Unlike the Ly-6C$^+$Ly-6G$^-$ cells that produce high levels of urea in the absence of iNOS, the Ly-6C$^+$Ly-6G$^+$ cells produced less urea in the absence of iNOS or NADPH oxidase (Figure 3c). These results indicate that in the absence of functional iNOS, arginase activity is differentially regulated between the monocytic (Ly-6C$^+$Ly-6G$^-$), granulocytic (Ly-6C$^+$Ly-6G$^+$) and macrophage-like (Ly-6C$^-$Ly-6G$^+$) subsets of myeloid cells.

MDSC-like cells have also been reported to take advantage of NADPH oxidase-dependent ROS mediated mechanisms to modulate inflammation. We next determined the significant cellular sources of superoxide production during airway inflammation. As shown in Supplementary Figure 5, at d3 following OVA challenge, ~80% of the DHE$^+$ cells from the wt lung tissue are Ly-6C$^-$Ly-6G$^+$ MDSC-like cells. Approximately 20% of the $O_2^{\cdot -}$-producing cells were F4/80$^-$Ly-6G$^+$ neutrophils or other cell types.

In an experimental model of *T. crassiceps* infection and in several models of cancer, arginase activity is also enhanced when iNOS activity is attenuated.[33, 34] The depletion of arginine due to activation of the arginase pathway leads to uncoupling of the NOS enzymes, which may result in consequent production of $O_2^{\cdot -}$.[35, 36] Consistent with this, approximately 70% of the lung Ly-6C$^-$Ly-6G$^+$ cells purified from iNOS$^{-/-}$ mice versus 2.6% from wt mice were positive for production of $O_2^{\cdot -}$ (DHE$^+$; Figure 3d, purple tracing **and** Supplementary Figure 6a, blue and pink tracings, respectively). DHE fluorescence was not detected in the NO-producing Ly-6C$^+$Ly-6G$^-$ subset from wt or iNOS$^{-/-}$ mice. The specificity of DHE fluorescence for NADPH oxidase-derived $O_2^{\cdot -}$ was confirmed in Ly-6C$^-$Ly-6G$^+$ cells from iNOS$^{-/-}$ mice cultured with the NADPH oxidase inhibitor diphenyleneiodonium (DPI) (Supplementary Figure 6a). In additional experiments using an assay that measured $O_2^{\cdot -}$ by the reduction of cytochrome c, we found that Ly-6C$^-$Ly-6G$^+$ cells from iNOS$^{-/-}$ mice generated 3-fold higher levels of $O_2^{\cdot -}$ compared to Ly-6C$^-$Ly-6G$^+$ cells from wt mice (Figure 3e). FACS analysis of BAL cells from OVA challenged iNOS$^{-/-}$ also showed a significant increase in the numbers of Ly-6G$^+$ DHE$^+$ cells (Supplementary Figure 6b). The granulocytic Ly-6C$^+$Ly-6G$^+$ cells produced undetectable levels of $O_2^{\cdot -}$ compared to the macrophage-like $O_2^{\cdot -}$-producing Ly-6C$^-$Ly-6G$^+$ cells or the NO-producing Ly-6C$^+$Ly-6G$^-$ cells (Figure 3d). These data demonstrate that the distinct myeloid cell subsets characterized here generate substantial quantities and specific profiles of reactive free radicals, giving them the potential to be important modulators of airway inflammatory responses.

In addition to their distinct free radical profiles, the profiles of cytokines they produced were different between the subsets. The Ly-6C$^+$Ly-6G$^-$ cell subset secreted substantial quantities of IL-6 and TNF-α (Figures 3f and 3g), both signature products of MDSC isolated from malignant tumors.[21, 22] In injury and chronic inflammation models, Ly-6G$^+$ macrophages participate in tissue repair and produce MMP-9.[37, 38] We detected VEGF, a factor whose expression is also associated with tissue repair, in increased concentrations in the supernatants of the arginase-expressing Ly-6C$^-$Ly-6G$^+$ cells compared to the NO-producing Ly-6C$^+$Ly-6G$^-$ subpopulation (Supplementary Figure 7a). VEGF levels were also increased in the BAL fluid at d3 after antigen challenge, with significantly higher levels noted in iNOS$^{-/-}$ compared to wt mice (Supplementary Figure 7b). Ly-6C$^-$Ly-6G$^+$ macrophages also produced MMP-9 in both cell lysates and culture supernatants, with a substantial portion being active MMP-9 (Supplementary Figures 8a and 8b). We hypothesize that the pro-oxidant phenotype of these cells may contribute to the creation of a pro-proteolytic environment, supporting repair associated with the resolution of the inflammatory process.

The iNOS and NADPH oxidase pathways regulate the accumulation of lung MDSC-like cells during asthmatic inflammation

To determine whether the free radical pathways contribute to the recruitment of the MDSC-like myeloid cell subsets to the lungs and to their potential to modulate the airway

inflammatory response, we first examined the time course of their accumulation in the lungs of antigen-challenged mice. The Ly-6C$^+$Ly-6G$^-$ myeloid cells were recruited in a biphasic fashion after antigen challenge, whereas the Ly-6C$^-$Ly-6G$^+$ cells were recruited in a monophasic fashion. Ly-6C$^+$Ly-6G$^-$ cells showed an initial peak (24±1.3-fold increase, $p<0.0001$, versus PBS-challenged controls) at d2 after i.n. OVA challenge of wt mice, followed by a second, larger peak (47±1.34-fold, $p<0.0001$) around d5 (Figure 4a). The Ly-6C$^-$Ly-6G$^+$ cells showed a single peak (10±1.97-fold, $p<0.0001$, versus PBS controls) coinciding with the decrease in Ly-6C$^+$Ly-6G$^-$ cells at d3 (Figure 4b). At d10 and d15, the numbers of both these subsets declined, but remained elevated above baseline. The numbers of Ly-6C$^+$Ly-6G$^+$ cells also showed a single peak after challenge with a 21±0.1-fold increase at d2 and 7±0.2-fold increase at d3, ($p<0.0001$ versus PBS controls).

Reduced numbers of Ly-6C$^+$Ly-6G$^-$ cells were observed throughout the course of the inflammatory response (Figure 4a) in the iNOS$^{-/-}$ mice. OVA challenge induced only a modest 2.7-fold increase in the numbers of iNOS$^{-/-}$ Ly-6C$^+$Ly-6G$^-$ cells (Supplementary Figure 9a). This correlated with reduced total infiltrating cells (Figure 1c) and lower levels of NO metabolites in the BAL fluid (Figure 1a). In contrast, a 12-fold increase in numbers of Ly-6C$^-$Ly-6G$^+$ cells induced by OVA challenge was observed in the lung tissue of iNOS$^{-/-}$ mice (Figure 4b). In contrast to the Ly-6C$^-$Ly-6G$^+$ cell subset, but similar to the Ly-6C$^+$Ly-6G$^-$ cell subset, the numbers of infiltrating Ly-6C$^+$Ly-6G$^+$ granulocytic MDSC-like cells were dramatically reduced in the lungs of OVA challenged iNOS$^{-/-}$ mice compared to the wt (Figure 4c).

To test whether $O_2^{\cdot -}$ was required for normal myeloid cell responses in the lungs of sensitized and challenged mice, we analyzed B6(Cg)-Ncf1m1J/J mice (referred to as p47m). This strain carries a mutation in the p47 subunit of NADPH oxidase that results in failure to produce $O_2^{\cdot -}$. The total numbers and percentages of lung Ly-6C$^+$Ly-6G$^-$ cells in p47m mice were dramatically increased by d2 after OVA challenge and remained elevated through d10 (Figure 5a and 5b). In contrast, the numbers of Ly-6C$^-$Ly-6G$^+$ cells were reduced in p47m mice (Figure 5a). Ly-6C$^+$Ly-6G$^+$ cells were also partially reduced (Supplementary Figure 9b) in p47m mice. A large fraction of the Ly-6C$^+$Ly-6G$^-$ cells in p47m mice also stained positive with NO indicator dye DAF-FM-DA (Figure 5b). The bioavailability of NO in asthmatic inflammation was also increased in the lungs of p47m mice. Not only were the numbers of the lung Ly-6C$^+$Ly-6G$^-$ cells significantly higher in p47m mice compared to wt, but lung Ly-6C$^+$Ly-6G$^-$ cells purified from p47m mice produced significantly higher levels of NO compared to wt (Figure 3a). The third subset of MDSC-like cells, the Ly-6C$^+$Ly-6G$^+$ granulocytic subset, produced low levels of NO in wt, iNOS$^{-/-}$ and p47 m mice compared to the NO-producing Ly-6C$^+$Ly-6G$^-$ (Figure 3a **and** Supplementary Figure 3).

Using iNOS$^{-/-}$ mice (Figures 3 **and** 4) and p47 mice (Figures 3, 5 **and** Supplementary Figure 9), we have shown that the numbers of lung infiltrating $O_2^{\cdot -}$-producing cells and NO-producing cells show a reciprocal relationship leading to consequent modulation of the levels of $O_2^{\cdot -}$ and NO and its metabolites (Figures 1 **and** 3). These data are consistent with the ability of $O_2^{\cdot -}$ *in vivo* to suppress the production of NO and to modulate the infiltration of Ly-6C$^+$Ly-6G$^-$ cells during the airway inflammatory response. Conversely, NO and its metabolites appear to be able to suppress the production of $O_2^{\cdot -}$ and the infiltration of Ly-6C$^-$Ly-6G$^+$ cells. Blockade of the iNOS pathway, therefore, would be expected to shift the free radical balance towards a $O_2^{\cdot -}$-enriched milieu in the lung, and blockade of the $O_2^{\cdot -}$-pathway would be expected to shift the balance towards a NO-enriched milieu.

These data suggest that the balance between reactive species generated by the linked free radical pathways can affect the differentiation, expansion or recruitment of MDSC-like cells into the site of the inflammatory response. Furthermore, they demonstrate that free radical

pathways differentially regulate the infiltration of monocytic (Ly-6C$^+$Ly-6G$^-$), granulocytic (Ly-6C$^+$Ly-6G$^+$) and macrophage-like (Ly-6C$^-$Ly-6G$^+$) subsets of myeloid cells.

Myeloid cell subsets can enhance or suppress T cell proliferation using the iNOS, arginase, and NADPH oxidase pathways

In view of the fact that tumor-derived MDSC inhibit T cell proliferative responses via their production of reactive free radicals[20] and given our findings that lung MDSC-like cell subsets generate distinct profiles of free radicals, we tested the ability of lung myeloid cell subsets to regulate T cell proliferative responses *in vitro*. When Ly-6C$^+$Ly-6G$^-$ myeloid cells sorted from the lungs of challenged wt mice were co-cultured at a 1:1 ratio with polyclonally activated naïve T cells (CD4$^+$CD25$^-$CD62L^{hi}CD44^{lo} cells sorted from the spleens of wt mice; Supplementary Figure 10a), T cell proliferation was suppressed by nearly 80% (Figure 6a). Co-culture with Ly-6C$^+$Ly-6G$^-$ cells from iNOS$^{-/-}$ mice did not elicit suppression of T cell proliferation. Furthermore, addition of 1400w, a specific inhibitor of iNOS, to the cultures largely reversed the inhibition of proliferation caused by wt Ly-6C$^+$Ly-6C$^-$cells (Figure 6a), indicating that NO generated by iNOS was a major mediator of the suppression. Since MDSC purified from malignant tumors also suppress T cell proliferation using the arginase pathway, we tested the effects of addition of nor-NOHA, a specific arginase pathway inhibitor, to the co-cultures. The ability of Ly-6C$^+$Ly-6G$^-$ MDSC-like cells to inhibit proliferation of wt naïve T cells was arginase-independent (Figure 6a). Additionally, Ly-6C$^+$Ly-6G$^-$ cells purified from lungs of OVA challenged p47m mice also suppressed the proliferation of naïve wt T cells (Figure 6a), with this inhibition completely reversed by 1400w but not by nor-NOHA. This confirmed that suppression of T cell proliferation by the monocytoid Ly-6C$^+$Ly-6G$^-$ MDSC-like subset was iNOS-dependent, but arginase-independent. Proliferation of OVA-specific OT-II transgenic CD4$^+$ T cells in the presence of OVA-pulsed antigen presenting cells was also inhibited by co-culture with purified wt lung Ly-6C$^+$Ly-6G$^-$ cells in a dose dependent manner (Supplementary Figure 10b).

Ly-6C$^+$Ly-6G$^+$ MDSC from human renal cell and lung cancers have been reported to inhibit T cell responses in an arginase-dependent fashion.[39, 40] Consistent with these studies, granulocytic Ly-6C$^+$Ly-6G$^+$ cells purified from the lungs of antigen-challenged wt mice showed substantial suppression of T cell proliferation via an arginase-mediated mechanism (manifested by partial reversal of the inhibition by co-culture with nor-NOHA) (Figure 6b). Interestingly, this myeloid cell population did not use iNOS or NADPH oxidase to modulate the proliferation of T cells, as inhibitors of these pathways did not reverse the T cell suppression (Figure 6b).

Strikingly, when the $O_2^{\cdot -}$-producing Ly-6C$^-$Ly-6G$^+$ myeloid cell subset was cultured together with naïve CD4$^+$ T cells, rather than suppressing proliferation, they induced a 33% increase in the T cell proliferative response (Figure 6c). Although modest, this enhancement of proliferation was statistically significant. The increase was dependent on the NADPH oxidase pathway because addition of catalase, SOD, or DPI to the cultures reduced T cell proliferation back to normal levels (Figure 6c). The reversal of enhanced T cell proliferation by catalase and DPI indicates that NADPH oxidase contributes importantly to the pro-proliferative effect of the Ly-6C$^-$Ly-6G$^+$ cells. It is likely that the NADPH oxidase that is expressed by the Ly-6C$^-$Ly-6G$^+$ cells is responsible for the accentuated T cell proliferation; however, these data cannot exclude the possibility that $O_2^{\cdot -}$ produced in an autocrine fashion by the responding T cells is responsible for the catalase and DPI effects, since activated T lymphocytes are known to express detectable NADPH oxidase.[41] Support for myeloid cells as the source of the biologically important $O_2^{\cdot -}$ comes from co-culture assays of naïve T cells from p47m mice together with Ly-6C$^-$Ly-6G$^+$ cells from $O_2^{\cdot -}$ competent and incompetent mice. These experiments have eliminated T cells as the source of $O_2^{\cdot -}$

because T cells from p47m mice respond with enhanced proliferation but only when co-cultured with $O_2^{\cdot -}$ competent Ly-6C$^-$Ly-6G$^+$ cells (data not shown). The pro-proliferative effect of these Ly-6C$^-$Ly-6G$^+$ cells was enhanced 2-fold when they were derived from iNOS$^{-/-}$ mice (Figure 6c). Since iNOS$^{-/-}$ Ly-6C$^-$Ly-6G$^+$ cells not only produce higher levels of $O_2^{\cdot -}$ but also showed increased arginase activity, we tested whether arginase contributed to the enhancement of T cell proliferation. We found that the ability of Ly-6C$^-$Ly-6G$^+$ cells from both C57BL/6 and iNOS$^{-/-}$ mice to accelerate T cell proliferation was also reversed by addition of nor-NOHA to the culture (Figure 6c), indicating an important role of arginase in the accentuation of T cell proliferation.

Lung myeloid regulatory cells attract T regulatory cells via CCL22

One mechanism by which MDSC in cancer suppress T cell responses is via enhancing the development of T regulatory (T_{reg}) cells.[31] Therefore, we first tested whether the suppressive NO-producing lung Ly-6C$^+$Ly-6G$^-$ cells enhance the *in vitro* differentiation of T_{reg} from naïve T cells. In co-cultures of Ly-6C$^+$Ly-6G$^-$ MDRC with naïve T cells (Supplementary Figure 11) we observed a very modest increase in the frequencies of T_{reg} (CD25$^+$Foxp3$^+$) at 3 days after culture, suggesting that lung MDRC may not be using this mechanism for suppression of T cell proliferation. Interestingly, there was a significant increase in CD25$^-$Foxp3$^+$ cells in the co-culture after 6 days **(**Supplementary Figure 11**)**. We have not evaluated the suppressive capacity of this population.

Next, we tested whether lung myeloid regulatory cells could also promote the migration of T_{reg} cells by secretion of CCL22, a CCR4 ligand that is chemotactic for these cells.[42] We observed high levels of CCL22 in the supernatants of cultured NO-producing Ly-6C$^+$Ly-6G$^-$ cells harvested at d2 after airway antigen challenge of wt mice but not iNOS$^{-/-}$ mice or in the supernatants of $O_2^{\cdot -}$-producing Ly-6C$^-$Ly-6G$^+$ cells (Figure 7a **and** Supplementary Figure 11). CCL22 was also detected in BAL fluid of OVA challenged wt and p47m mice at times when NO-producing Ly-6C$^+$Ly-6G$^-$ cells were present in the lung (Supplementary Table I). Production of CCL22 by Ly-6C$^+$Ly-6G$^-$ cells from iNOS$^{-/-}$ mice was low or undetectable. Additionally, TGF-β1 and IL-10, cytokines known to contribute to the differentiation, development and function of T_{reg} cells, were increased in supernatants from cultures of wt Ly-6C$^+$Ly-6G$^-$ cells (Figures 7b and 7c) compared to Ly-6C$^-$Ly-6G$^+$ or Ly-6C$^+$Ly-6G$^-$ cells.

Using a transwell migration assay, we investigated whether Ly6C$^+$Ly-6G$^-$ cells induced the *in vitro* chemotaxis of CD4$^+$CD25$^+$Foxp3/GFP$^+$ T_{reg} cells in a CCL22-dependent fashion. Supernatants from Ly-6C$^+$Ly-6G$^-$ cells, but not from Ly-6C$^-$Ly-6G$^+$ cells, promoted chemotaxis of T_{reg} cells (Figure 7d). Chemotaxis of naïve CD4$^+$ T cells did not occur (data not shown). Addition of neutralizing anti-CCL22 antibody blocked the chemotaxis of T_{reg} cells induced by Ly-6C$^+$Ly-6G$^-$ cell culture supernatants. Consistent with these data, the frequency of lung T_{reg} cells was reduced in the iNOS$^{-/-}$ mice compared to wt, and substantially increased in p47m mice (Figures 7e and 7f). Together, these data suggest that lung Ly-6C$^+$Ly-6G$^-$ cells, in addition to the direct action of NO on T cell proliferation (Figure 6), also can suppress T cell responses in an NO-dependent, CCL22-dependent fashion that involves the recruitment and accumulation of T_{reg} cells in the lung.

Modulation of AHR by myeloid-derived cell subsets

To determine whether myeloid cell subsets regulate allergen-induced AHR, we first determined the baseline airway responses to increasing concentrations of methacholine in OVA-sensitized wt, iNOS$^{-/-}$ and p47m mice challenged with OVA. In sensitized wt mice, OVA challenge resulted in methacholine hyper-responsiveness (Figure 8a). AHR was increased in the iNOS$^{-/-}$ mice and reduced in p47m mice (Figure 8a). Sensitized and

challenged wt mice that received intratracheal (i.t.) adoptive transfer of 10^5 Ly-6C$^+$Ly-6G$^-$ cells purified from asthmatic wt mice showed significantly reduced AHR (Figure 8b). Intratracheal adoptive transfer of Ly-6C$^+$Ly-6G$^-$ cells purified from lungs of iNOS$^{-/-}$ donors modestly enhanced, rather than reduced AHR (Figure 8b), indicating that iNOS-derived NO is critical for the suppression of AHR induced by wt Ly-6C$^+$Ly-6G$^-$ cells. In contrast, adoptive transfer of wt $O_2^{\cdot -}$-producing Ly-6C$^-$Ly-6G$^+$ cells caused a substantial increase in AHR following airway antigen challenge. This effect was dramatically more pronounced in recipients of Ly-6C$^-$Ly-6G$^+$ cells from iNOS$^{-/-}$ donors, further identifying iNOS-derived NO as a suppressor of AHR and supporting a role for $O_2^{\cdot -}$ as an effector of hyper-responsiveness. Modulation of antigen-induced AHR was not observed with i.t. transfer of PBS or of *in vitro* differentiated bone marrow-derived CD11c$^+$ dendritic cells (BMDC) into wt recipients (Figure 8b). Similar patterns of myeloid cell-mediated modulation of airway elastance and tissue resistance were also observed following i.t. transfer of the different myeloid cells subsets (data not shown).

To further test the contribution of $O_2^{\cdot -}$ produced by wt Ly-6C$^-$Ly-6G$^+$ in AHR, we treated the cells with DPI to inhibit their NADPH oxidase-mediated production of $O_2^{\cdot -}$, then transferred them i.t. into OVA-sensitized wt or p47m mice 2 days before OVA challenge. While the i.t. transfer of untreated wt Ly-6C$^-$Ly-6G$^+$ cells into asthmatic wt and p47m mice significantly increased AHR (Figure 8c), AHR was inhibited as a result of i.t. transfer of wt Ly-6C$^-$Ly-6G$^+$ cells treated with the NADPH oxidase inhibitor DPI. Consistent with this observation, the transfer of wt Ly-6C$^-$Ly-6G$^+$ cells into OVA-sensitized wt or p47m mice also significantly increased levels of OVA specific IgE in both BAL fluid and serum as well as levels of Muc5Ac protein in lung tissue compared to OVA challenged wt or p47m mice **(**Supplementary Figure 13**).** Interestingly, transfer of wt Ly-6C$^-$Ly-6G$^+$ cells treated with DPI resulted in reduction of OVA specific IgE well below the BAL fluid IgE levels in OVA challenged mice. Muc5Ac protein expression in lung tissue was also reduced following transfer of wt Ly-6C$^-$Ly-6G$^+$ cells treated with DPI. These data further confirmed the direct role of $O_2^{\cdot -}$-producing Ly-6C$^-$Ly-6G$^+$ cells in AHR and emphasize the significant contribution of free radical pathways to airway inflammation and AHR.

Intratracheal transfer of NO-producing wt Ly-6C$^+$Ly-6G$^-$ cells into OVA-sensitized and challenged iNOS$^{-/-}$ mice down-modulated the abnormally high AHR observed in this mouse strain (Figure 8d), suggesting that iNOS-derived NO normally contributes in avoiding excessive AHR. Suppression of AHR was not observed after adoptive transfer of BMDC or of PBS alone. Consistent with their effects on airway responsiveness, lung Ly-6C$^+$Ly-6G$^-$ cells from iNOS$^{-/-}$ mice secreted elevated levels of IL-13 in culture (Supplementary Figure 14), suggesting that NO may modulate expression of Th2 cytokines that are associated with AHR. Although IL-13 has generally been thought to be a T cell-derived cytokine, our findings support Ly-6C$^+$Ly-6G$^-$ MDRC in addition to mast cells and eosinophils as myeloid lineage sources of this Th2− and AHR-associated cytokine. Altogether, our data suggest a critical role for Ly-6C$^+$Ly-6G$^-$ cells as endogenous regulators of AHR via iNOS-dependent mechanisms, and Ly-6C$^-$Ly6G$^+$ myeloid cells as effectors of $O_2^{\cdot -}$-dependent exacerbations of AHR.

DISCUSSION

The identification of three distinct myeloid cell subsets with potent immunomodulating functions in the lungs of allergen sensitized and challenged mice reveals a previously unrecognized network of innate cells that can modulate Th2 cell-dependent tissue inflammatory processes such as asthma. These myeloid cell populations share surface expression of the Gr-1, CD11b and F4/80 antigens suggesting that they are lineage related. They differ, however, in their expression of the Ly-6C and Ly-6G antigens and in their

profiles of reactive free radicals and cytokines. The subsets defined as Ly-6C^{+}Ly-6G^{-} (showing monocytic morphology) and Ly-6C^{+}Ly-6G^{+} (with granulocyte morphology) both show potent anti-inflammatory activities and resemble MDSC that suppress T cell function in cancer. The monocytoid Ly-6C^{+}Ly-6G^{-} cells appear to be phenotypically similar also to the Ly-6C^{hi} monocytes recruited in the healing myocardium and models of Listeria infection,[43] but are quite distinct from those participating in Leishmania infection.[44] Importantly, the Ly-6C^{+}Ly-6G^{-} cells identified in this study also show potent activity to down-modulate asthmatic AHR. In contrast, the Ly-6C^{-}Ly-6G^{+} subset (with macrophage morphology) show proinflammatory activities that exacerbate key aspects of the asthmatic response including AHR. Because these three subsets share lineage markers, but are not monomorphic in their suppressive function, we propose that they be designated myeloid-derived *regulatory* cells (MDRC) to acknowledge both their immune up-regulating and immune down-modulating functions.

MDRC accumulate early in the response to airway antigen challenge, with all three subsets present by d2 in wt mice. The Ly-6C^{+}Ly-6G^{-} cells generate micromolar concentrations of NO via iNOS without detectable $O_2^{\cdot -}$ and express low levels of arginase activity. The initial wave of NO-producing Ly-6C^{+}Ly-6G^{-} cells disappeared by d3, the time of peak infiltration by both Ly-6C^{-}Ly-6G^{+} cells and eosinophils. Although there was an increase in apoptosis among the Ly-6C^{+}Ly-6G^{-} cells at d2 prior to their disappearance (Supplementary Figure 15), we cannot exclude that emigration from the lungs, changes in their surface phenotype, or non-apoptotic cell turnover also contributed to their attrition at this time. A second wave of Ly-6C^{+}Ly-6G^{-} cells peaked at d5, associated with decay of the eosinophil response and reduction in the numbers of Ly-6C^{-}Ly-6G^{+} cells. These cells resemble MDSC in their ability to suppress T cell proliferation in an iNOS-dependent fashion. Suppression of T cell proliferation was independent of arginase and NADPH oxidase, consistent with the low arginase activity and undetectable $O_2^{\cdot -}$ production by this cell subset. Strikingly, after i.t. adoptive transfer into sensitized and antigen challenged wt mice, these NO-producing cells potently suppressed antigen-induced AHR. The central role of iNOS-dependent NO on the accumulation and function of Ly-6C^{+}Ly-6G^{-} cells was underscored by their dramatically reduced numbers in the lungs of challenged iNOS$^{-/-}$ mice and the failure of Ly-6C^{+}Ly-6G^{-} cells purified from iNOS$^{-/-}$ mice to suppress AHR after adoptive transfer into challenged wt mice. $O_2^{\cdot -}$ produced by the NADPH oxidase pathway appeared to play a counter-regulatory role for these NO-producing cells, with their numbers substantially increased in the lungs of sensitized and challenged p47m mice (Figures 4 **and** 5).

The important impact of the balance of anti-inflammatory and pro-inflammatory free radicals on physiological responses in the lung is particularly evident in the AHR response. iNOS$^{-/-}$ mice, which have reduced NO-producing Ly-6C^{+}Ly-6G^{-} cells in the airway and increased $O_2^{\cdot -}$-producing Ly-6C^{-}Ly-6G^{+} cells, show increased AHR, whereas p47m mice, which have the reciprocal pattern of NO- and $O_2^{\cdot -}$-producing cells, show reduced AHR. Although the overall cellular infiltration is significantly reduced in the iNOS$^{-/-}$ mice during asthmatic inflammation compared to wt mice, AHR was significantly higher, thus un-linking AHR from the overall level of cell infiltration. The lack of correlation between levels of cellular infiltration and degree of AHR was consistent with our observation that despite significantly reduced AHR in p47m mice, the overall level of cellular infiltration was much higher in this strain compared to asthmatic wt and iNOS$^{-/-}$ mice (Supplementary Figure 16). Importantly, intratracheal administration of Ly-6C^{-}Ly-6G^{+} MDRC purified from wt and iNOS$^{-/-}$ mice into sensitized and antigen challenged wt mice exacerbated AHR. Our studies of Ly-6C^{-}Ly-6G^{+} cells extracted from the lungs of sensitized and challenged wt mice showed that they consistently expressed $O_2^{\cdot -}$, but at quite modest levels. Despite the modest levels of $O_2^{\cdot -}$-produced by the wt Ly-6C^{-}Ly-6G^{+} MDRC, they elicited physiologically significant responses by increasing OVA specific IgE levels in the airway and serum as well

as MUC5Ac protein levels in the lung tissue (Supplementary Figure 13). It remains possible that these cells express higher levels of $O_2^{\cdot -}$ *in vivo* under the influence of signals that are lost when the cells are removed from their natural microenvironment. Regardless, our data indicate that the ability of these cells to produce $O_2^{\cdot -}$ is physiologically important. This is shown by the fact that inhibition of their ability to produce $O_2^{\cdot -}$ by treatment with DPI blocked their augmentation of the pro-inflammatory response, their enhancement of AHR and their increase in expression of OVA-specific IgE and Muc5Ac. These results support a role for $O_2^{\cdot -}$, and perhaps arginase and other mediators produced by these cells, in regulating levels of IgE and the airway physiological response. The suppression of AHR in the p47m mice and the known efficacy of SOD[45] or SOD mimetics[46] as inhibitors of AHR, also supports $O_2^{\cdot -}$ as a central mediator of AHR. Unexplained, however, is the lack of attenuation of the asthmatic response by over-expression of catalase in mouse airways.[47] We have not ruled out peroxynitrite-mediated regulation of mucin expression in this study. Future studies will determine whether the reduced AHR and reduced mucin expression observed in p47m compared to wt mice is due to a direct result of the reduced levels of $O_2^{\cdot -}$ in the airways, or from overall reduction in levels of peroxynitrite formation from downstream interactions of $O_2^{\cdot -}$ with NO.

The pro-inflammatory activity of $O_2^{\cdot -}$-producing Ly-6C$^-$Ly-6G$^+$ cells from lungs of both wt and iNOS$^{-/-}$ mice was underscored by their ability to enhance proliferation of polyclonally activated T cells *in vitro* in a $O_2^{\cdot -}$-dependent fashion. This was consistent with the known roles for hydrogen peroxide and NADPH oxidase-derived $O_2^{\cdot -}$ in cell proliferation during inflammation.[48, 49] The arginase pathway may cooperate importantly with pathways that produce reactive oxygen species and other endogenous signals in modulating proinflammatory responses in the airways since the proliferation-enhancing activity of Ly-6C$^-$Ly-6G$^+$ MDRC was attenuated by the arginase inhibitor nor-NOHA. Deficiency of iNOS can promote activation of arginase and production of urea and polyamines, which support proliferative responses and tissue repair.[10, 50] In addition, activation of arginase can deplete local L-Arg.[10] Even in the absence of functional iNOS, this can lead to uncoupling of eNOS and nNOS, causing production of $O_2^{\cdot -}$. Thus, deficiency of iNOS can lead to enhanced $O_2^{\cdot -}$ production by a variety of mechanisms.

In addition to the direct action of the NO-producing Ly-6C$^+$Ly-6G$^-$ cells on T cell proliferation, we identified substantial numbers of Foxp3$^+$ T_{reg} cells in the lungs of challenged mice when the NO-producing cells were prevalent (Figures 7e and 7f). The Ly-6C$^+$Ly-6G$^-$ cells secreted CCL22 in an iNOS-dependent fashion, and promoted CCL22-dependent chemotaxis of T_{reg} cells *in vitro* (Figure 7d). Ly-6C$^+$Ly-6G$^-$ MDRC from p47m mice produced more CCL22 than did wt Ly-6C$^+$Ly-6G$^-$ cells, and p47m mice showed increased numbers of T_{reg} cells in the lungs of challenged animals supporting a role for $O_2^{\cdot -}$ in limiting the participation of T_{reg} cells in the tissue inflammatory response. It remains to be determined whether, in addition to supporting their chemotaxis to the lung, Ly-6C$^+$Ly-6G$^-$ MDRC can also support the *de novo* differentiation of T_{reg} cells from naïve precursors, as has been described for NO-producing MDSC.[20-22, 31] Their cytokine expression profile, with substantial production of IL-6, TNF-α, CCL22, TGF-β1 and IL-10, is characteristic of MDSC[51] with phenotypic characteristics of both M1 and M2 macrophages, and further supports their role in promoting T_{reg} cell responses.

The granulocytic Ly-6C$^+$Ly-6G$^+$F4/80$^+$ cells described here which infiltrate the lung in significantly fewer numbers differ from conventional circulating neutrophils by virtue of their larger size manifested by increased forward light scatter detected by FACS (data not shown). Although granulocytes may express F4/80, especially when they transdifferentiate towards the macrophage lineage,[52] the relationship between Ly-6C$^+$Ly-6G$^+$F4/80$^+$ cells and conventional F4/80$^-$ neutrophils remains to be determined. These granulocytic

Ly-6C$^+$Ly-6G$^+$ cells, however, are similar to granulocytic MDSC that are immunosuppressive in tumor-bearing mice and humans. Like granulocytic MDSC, they suppressed polyclonal T cell proliferation in an arginase-dependent, but iNOS- and NADPH oxidase-independent mechanism. It is unclear whether the mechanism of suppression involves release of arginase and subsequent depletion of local L-Arg. Arginase is important for T cell suppression by wt Ly-6C$^+$Ly-6G$^+$ MDRC; however, unlike the $O_2^{\cdot -}$-producing Ly-6C$^-$Ly-6G$^+$ subset, arginase activity is not increased in iNOS-deficient Ly-6C$^+$Ly-6G$^+$ cells, suggesting that these granulocytic MDRC use alternate strategies to regulate the free radical pathways. Interestingly, we could detect neither NO nor $O_2^{\cdot -}$ in isolated Ly-6C$^+$Ly-6G$^+$ cells. This has limited our ability to investigate the contribution of free radical mechanisms to their impact on inflammatory responses *in vivo*. Of additional interest, this was the only MDRC subset that showed detectable evidence of tyrosine nitration (data not shown). Because this MDRC subset is present in only small numbers in the lung, characterization of their impact *in vivo* has been difficult and will require additional study.

Functional iNOS is required both to establish normal numbers of anti-inflammatory Ly-6C$^+$Ly-6G$^-$ MDRC and to prevent excessive expansion of pro-inflammatory Ly-6C$^-$Ly-6G$^+$ MDRC. In contrast, functional NADPH oxidase is required to establish normal numbers of Ly-6C$^-$Ly-6G$^+$ MDRC and to prevent excessive expansion of NO-producing Ly-6C$^+$Ly-6G$^-$ cells. These observations demonstrate that there is an intricate balance between these anti-inflammatory and pro-inflammatory MDRC subsets, and suggest that the major free radical products of these cells are key mediators modulating these actions. As shown in Figure 9, our studies establish that in addition to the known role of MDSC in cancer and chronic infectious and autoimmune diseases, myeloid-derived regulatory cells are important mediators of tissue inflammatory diseases such as asthma. Both pro- and anti-inflammatory MDRC affect T cell activation. Additionally, NO-producing MDRC have the potential to recruit T_{reg} cells as a consequence of their expression of CCL22. Finally, we demonstrate that in addition to their ability to modulate local T cell responses, $O_2^{\cdot -}$-producing MDRC can enhance and NO-producing MDRC can suppress the AHR that contributes importantly to the pathophysiology of asthma.

The impact of free radicals or their metabolites on the development and accumulation of the MDRC subsets defined here suggests that the boundaries between M1, M2 and other myeloid cell phenotypes are not rigidly defined. It is unknown whether the MDRC subsets described here are transient, intermediate differentiation states controlled by the overall free radical milieu, or rather represent end-points of lineage differentiation, with changes in the proinflammatory set point requiring removal of the committed cells and their replacement with newly differentiating regulatory cells. We hypothesize that changes in myeloid cell polarity may set the pro-inflammatory/anti-inflammatory rheostat in antigen-driven tissue immune responses, and that manipulation of this plastic system could afford new opportunities for treatment of inflammatory diseases, including those of the lung. Prior studies have focused on the suppressive action of MDSC, with little or no attention to the pro-inflammatory arm of this myeloid regulatory cell system. Our findings provide the substrate for a systematic investigation of analogous myeloid regulatory subsets in other inflammatory disorders, especially in human asthma, with the aim of better understanding the controversial role for nitric oxide, superoxide and other free radicals in the regulation of the inflammatory responses and disturbed airway physiology of this disorder. Furthermore, pharmacologic interventions that include NO mimetics or superoxide scavengers may prove valuable in the treatment of asthma.

MATERIALS AND METHODS

Mice

C57BL/6, B6(Cg)-Ncf1m1J/J and iNOS$^{-/-}$ mice were from The Jackson Laboratory, Bar Harbor, ME. OT-II mice were provided by Paul Allen, Washington University, St. Louis, MO, and *Foxp3*^{gfp} mice by Alexander Rudensky, Memorial Sloan-Kettering Cancer Center, New York, NY. Mice 6-8 weeks of age were housed under pathogen-free conditions in micro-isolator cages and experiments were approved by the Institutional Animal Care and Use Committee of the University of Alabama at Birmingham.

Experimental allergic airway inflammation

Mice were sensitized by intraperitoneal (i.p.) injection on d0 and d7 with 50 μg of alum-precipitated OVA (Grade VII, Sigma Chemical, St. Louis, MO; less than 1 ng LPS/mg) as previously described[2]. On d14, under anesthesia with Isoflurane (Schering-Plough Animal Health, Union, NJ), mice were challenged intranasally (i.n.) with 0.03 ml 0.03% OVA in PBS or PBS alone. At various times after challenge, mice were euthanized and BAL fluid and lung tissue were harvested. (See further details in supplementary methods).

Measurements of NO, arginase activity and superoxide

DAF-FM-DA (Molecular Probes, Eugene, OR), an intracellular indicator for NO, and the Griess assay were used to detect and measure metabolites of NO. Arginase activity was estimated by measuring urea with the Quantichrom Urea Assay kit (DIUR-500; BioAssay Systems, Hayward, CA). Superoxide was detected by FACS using the fluorescent indicator DHE (Dihydroxyethidium, Molecular Probes, Eugene, OR) and quantitated by spectrophotometric measurements of cytochrome c reduction (See further details in supplementary methods).

Measurement of T cell suppressive function

CD4$^+$CD25$^-$ splenic T cells purified from OT-II CD45.1 mice by FACS (10^7 cells/ml) were incubated with 1μM CFSE (Molecular Probes) for 15 min at RT in serum-free RPMI 1640. Labeling was stopped by addition of an equal volume of heat-inactivated FBS followed by several washes in complete R-10 medium (RPMI 1640 containing 2 mM L-glutamine, 10 μg/ml penicillin-streptomycin, 25 μM 2-mercaptoethanol, 0.1 mM non-essential amino acids (Life Technologies, Gaithersburg, MD) and 10% heat-inactivated FBS (Hyclone, Logan, UT)). Bone marrow-derived dendritic cells (BMDC)[53] were purified and incubated overnight at 37°C with 1 μg/ml OVA$^{323\text{-}339}$ peptide. 10^5 viable BMDC were then co-cultured with 10^5 CFSE-labeled OT-II T cells and 10^5 cells of purified MDRC subsets. After d3, proliferation of the T cells was measured by flow cytometry as CFSE dilution. Alternatively, subsets of purified MDRC were co-cultured for 48h with naïve CD4$^+$ T cells in a 1:1 ratio following activation with anti-CD3 and anti-CD28 antibodies (0.75 μg & 4 μg/ml respectively; BD Pharmingen, San Diego, CA). ^{3}H-thymidine (1 μCi/well) was added and incorporation of ^{3}H was determined 16h later. To determine the roles of iNOS, NADPH oxidase, $O_2^{\cdot -}$, and arginase as modulators of T cell proliferation, 500 nM 1400w (Cayman Chemical, Ann Arbor, MI), 10 μM diphenyleneiodonium (DPI, Tocris Bioscience, Ellisville, MO), 1000 U/ml catalase (Sigma), 1000 U/ml superoxide dismutase (SOD) (Sigma), or 20 μM nor-NOHA (Cayman Chemical, Ann Arbor, MI) was added at the start of the cultures.

Adoptive transfer of MDRC

MDRC populations that were Gr-1$^+$CD11b$^+$F4/80$^+$ and either Ly-6C$^+$Ly-6G$^-$ or Ly-6C$^-$Ly-6G$^+$ were purified by FACS from the lungs of sensitized mice at d2 or d3 after

antigen challenge. MDRC subsets (10^5 in 30 μl sterile PBS) were adoptively transferred i.t. into anesthetized mice that had been sensitized i.p. 12d previously with OVA. Two days later, these mice were challenged i.n. with OVA (30 μl of 0.03%) (See additional details in supplementary methods).

Measurement of AHR

Airway resistance, lung tissue resistance, and lung elastance were measured in response to increasing concentrations of inhaled aerosolized methacholine (0-50 mg/ml in water).[54] Mice were anesthetized with ketamine (10 mg/kg i.p.) followed by pancuronium bromide (2.0 mg/kg). After insertion of an 18G tracheostomy catheter, the mice were mechanically ventilated at 160 breaths/min with a tidal volume of 0.2 ml, and a positive end-expiratory pressure of 2-4 cm.H2O using a Flexi Vent apparatus (SCIREQ, Montreal, Canada). Tissue resistance was computed continuously over the period of 20 sec to 6 min and an average of 12 readings at 30 s intervals was used for calculations. Mean values of tissue resistance ± SD are plotted.

Statistical analysis

Experiments were performed at least 3 times. Results are expressed as means ± SEM unless otherwise specified. Student's t-test, ANOVA with Tukey post-test, and two-way ANOVA with repeated measures and Bonferroni correction were used for comparisons. All results were considered significant at $p<0.05$.

Supplementary Material

Refer to Web version on PubMed Central for supplementary material.

Acknowledgments

The authors thank Meiqin Zeng for expert technical assistance and Kathy May for management of the animal colony used to support this work. We gratefully acknowledge Dr. Hubert Tse for providing p47m mice to carry out adoptive transfer experiments. We also acknowledge helpful comments from Dr. Jack Lancaster, Dr. Carlene Zindl, Dr. Kelly M. McNagny, and Dr. Jillian Wohler. Support for these studies was provided by NIH grants 5T32HL007553 (JD), 5T32AI007051 (JD), 1F32HL095341 (JD), 5P01HL073907 (DC), 5R01HL075465 (LS), 5R01HL062221 (EA), 1R01GM087748 (EA), and 2R01HL076206 (EA).

References

1. Djukanovic R, et al. Mucosal inflammation in asthma. Am. Rev. Respir. Dis. 1990; 142:434–457. [PubMed: 2200318]
2. Randolph DA, Stephens R, Carruthers CJL, Chaplin DD. Cooperation between Th1 and Th2 cells in a murine model of eosinophilic airway inflammation. J. Clin. Invest. 1999; 104:1021–1029. [PubMed: 10525040]
3. Schroder NW, Maurer M. The role of innate immunity in asthma: leads and lessons from mouse models. Allergy. 2007; 62:579–590. [PubMed: 17508961]
4. Calhoun WJ, Reed HE, Moest DR, Stevens CA. Enhanced superoxide production by alveolar macrophages and air-space cells, airway inflammation, and alveolar macrophage density changes after segmental antigen bronchoprovocation in allergic subjects. Am. Rev. Respir. Dis. 1992; 145:317–325. [PubMed: 1310575]
5. Dupont LJ, Rochette F, Demedts MG, Verleden GM. Exhaled nitric oxide correlates with airway hyperresponsiveness in steroid-naive patients with mild asthma. Am. J. Respir. Crit. Care Med. 1998; 157:894–898. [PubMed: 9517608]
6. Folkerts G, Kloek J, Muijsers RB, Nijkamp FP. Reactive nitrogen and oxygen species in airway inflammation. Eur. J. Pharmacol. 2001; 429:251–262. [PubMed: 11698045]

7. Robbins RA, Hadeli K, Nelson D, Sato E, Hoyt JC. Nitric oxide, peroxynitrite, and lower respiratory tract inflammation. Immunopharmacology. 2000; 48:217–221. [PubMed: 10960660]
8. Chaturvedi R, et al. L-arginine availability regulates inducible nitric oxide synthase-dependent host defense against Helicobacter pylori. Infect. Immun. 2007; 75:4305–4315. [PubMed: 17562760]
9. De Sanctis GT, et al. Contribution of nitric oxide synthases 1, 2, and 3 to airway hyperresponsiveness and inflammation in a murine model of asthma. J. Exp. Med. 1999; 189:1621–1630. [PubMed: 10330441]
10. Maarsingh H, Zaagsma J, Meurs H. Arginine homeostasis in allergic asthma. Eur. J. Pharmacol. 2008; 585:375–384. [PubMed: 18410920]
11. Maarsingh H, de Boer J, Kauffman HF, Zaagsma J, Meurs H. Heparin normalizes allergen-induced nitric oxide deficiency and airway hyperresponsiveness. Br. J. Pharmacol. 2004; 142:1293–1299. [PubMed: 15265801]
12. Lensmar C, Katchar K, Eklund A, Grunewald J, Wahlstrom J. Phenotypic analysis of alveolar macrophages and lymphocytes following allergen inhalation by atopic subjects with mild asthma. Respir. Med. 2006; 100:918–925. [PubMed: 16202577]
13. Ckless K, et al. Inhibition of arginase activity enhances inflammation in mice with allergic airway disease, in association with increases in protein S-nitrosylation and tyrosine nitration. J. Immunol. 2008; 181:4255–4264. [PubMed: 18768883]
14. Peters EA, Hiltermann JT, Stolk J. Effect of apocynin on ozone-induced airway hyperresponsiveness to methacholine in asthmatics. Free Radic. Biol. Med. 2001; 31:1442–1447. [PubMed: 11728816]
15. Komlósi ZI, et al. Lipopolysaccharide exposure makes allergic airway inflammation and hyper-responsiveness less responsive to dexamethasone and inhibition of iNOS. Clin. Exp. Allergy. 2006; 36:951–959. [PubMed: 16839411]
16. Maarsingh H, et al. Arginase inhibition protects against allergen-induced airway obstruction, hyperresponsiveness, and inflammation. Am. J. Respir. Crit. Care Med. 2008; 178:565–573. [PubMed: 18583571]
17. Zimmermann N, Rothenberg ME. The arginine-arginase balance in asthma and lung inflammation. Eur. J. Pharmacol. 2006; 533:253–262. [PubMed: 16458291]
18. Satoh M, et al. NAD(P)H oxidase and uncoupled nitric oxide synthase are major sources of glomerular superoxide in rats with experimental diabetic nephropathy. Am. J. Physiol. Renal. Physiol. 2005; 288:F1144–1152. [PubMed: 15687247]
19. Morel F, Doussiere J, Vignais PV. The superoxide-generating oxidase of phagocytic cells. Eur. J. Biochem. 1991; 201:523–546. [PubMed: 1657601]
20. Serafini P, Borrello I, Bronte V. Myeloid suppressor cells in cancer: recruitment, phenotype, properties, and mechanisms of immune suppression. Semin. Cancer Biol. 2006; 16:53–65. [PubMed: 16168663]
21. Gabrilovich DI, Nagaraj S. Myeloid-derived suppressor cells as regulators of the immune system. Nat. Rev. Immunol. 2009; 9:162–174. [PubMed: 19197294]
22. Ostrand-Rosenberg S, Sinha P. Myeloid-derived suppressor cells: linking inflammation and cancer. J. Immunol. 2009; 182:4499–4506. [PubMed: 19342621]
23. Zhu B, et al. CD11b+Ly-6C(hi) suppressive monocytes in experimental autoimmune encephalomyelitis. J. Immunol. 2007; 179:5228–5237. [PubMed: 17911608]
24. Haile LA, et al. Myeloid-derived suppressor cells in inflammatory bowel disease: a new immunoregulatory pathway. Gastroenterology. 2008; 135:871–881. [PubMed: 18674538]
25. Marhaba R, et al. The importance of myeloid-derived suppressor cells in the regulation of autoimmune effector cells by a chronic contact eczema. J. Immunol. 2007; 179:5071–5081. [PubMed: 17911592]
26. Hohl TM, et al. Inflammatory monocytes facilitate adaptive CD4 T cell responses during respiratory fungal infection. Cell Host Microbe. 2009; 6:470–481. [PubMed: 19917501]
27. Goni O, Alcaide P, Fresno M. Immunosuppression during acute Trypanosoma cruzi infection: involvement of Ly6G (Gr1(+))CD11b(+)immature myeloid suppressor cells. Int. Immunol. 2002; 14:1125–1134. [PubMed: 12356678]

28. Hanson EM, Clements VK, Sinha P, Ilkovitch D, Ostrand-Rosenberg S. Myeloid-derived suppressor cells down-regulate L-selectin expression on CD4+ and CD8+ T cells. J. Immunol. 2009; 183:937–944. [PubMed: 19553533]
29. Bratt JM, et al. Arginase enzymes in isolated airways from normal and nitric oxide synthase-2 knockout mice exposed to ovalbumin. Toxicol. Appl. Pharmacol. 2009; 234:273–280. [PubMed: 19027033]
30. Gueders MM, et al. Mouse models of asthma: a comparison between C57BL/6 and BALB/c strains regarding bronchial responsiveness, inflammation, and cytokine production. Inflamm. Res. 2009; 58:845–854. [PubMed: 19506803]
31. Huang B, et al. Gr-1+CD115+ immature myeloid suppressor cells mediate the development of tumor-induced T regulatory cells and T-cell anergy in tumor-bearing host. Cancer Res. 2006; 66:1123–1131. [PubMed: 16424049]
32. Dietlin TA, et al. Mycobacteria-induced Gr-1+ subsets from distinct myeloid lineages have opposite effects on T cell expansion. J. Leukoc. Biol. 2007; 81:1205–1212. [PubMed: 17307863]
33. Brys L, et al. Reactive oxygen species and 12/15-lipoxygenase contribute to the antiproliferative capacity of alternatively activated myeloid cells elicited during helminth infection. J. Immunol. 2005; 174:6095–6104. [PubMed: 15879104]
34. Bronte V, et al. IL-4-Induced arginase 1 suppresses alloreactive T cells in tumor-bearing mice. J. Immunol. 2003; 170:270–278. [PubMed: 12496409]
35. Xia Y, Roman LJ, Masters BS, Zweier JL. Inducible nitric-oxide synthase generates superoxide from the reductase domain. J. Biol. Chem. 1998; 273:22635–22639. [PubMed: 9712892]
36. Xia Y, Tsai AL, Berka V, Zweier JL. Superoxide generation from endothelial nitric-oxide synthase. A Ca2+/calmodulin-dependent and tetrahydrobiopterin regulatory process. J. Biol. Chem. 1998; 273:25804–25808. [PubMed: 9748253]
37. Cortez-Retamozo V, et al. Real-time assessment of inflammation and treatment response in a mouse model of allergic airway inflammation. J. Clin. Invest. 2008; 118:4058–4066. [PubMed: 19033674]
38. Nahrendorf M, et al. The healing myocardium sequentially mobilizes two monocyte subsets with divergent and complementary functions. J. Exp. Med. 2007; 204:3037–3047. [PubMed: 18025128]
39. Rodriguez PC, et al. Arginase I-Producing Myeloid-Derived Suppressor Cells in Renal Cell Carcinoma Are a Subpopulation of Activated Granulocytes. Cancer Res. 2009; 69:1553–1560. [PubMed: 19201693]
40. Youn J-I, Nagaraj S, Collazo M, Gabrilovich DI. Subsets of myeloid-derived suppressor cells in tumor-bearing mice. J. Immunol. 2008; 181:5791–5802. [PubMed: 18832739]
41. Jackson SH, Devadas S, Kwon J, Pinto LA, Williams MS. T cells express a phagocyte-type NADPH oxidase that is activated after T cell receptor stimulation. Nat. Immunol. 2004; 5:818–827. [PubMed: 15258578]
42. Mizukami Y, et al. CCL17 and CCL22 chemokines within tumor microenvironment are related to accumulation of Foxp3+ regulatory T cells in gastric cancer. Int. J. Cancer. 2008; 122:2286–2293. [PubMed: 18224687]
43. Jia T, et al. Additive roles for MCP-1 and MCP-3 in CCR2-mediated recruitment of inflammatory monocytes during Listeria monocytogenes infection. J. Immunol. 2008; 180:6846–6853. [PubMed: 18453605]
44. De Trez C, et al. iNOS-producing inflammatory dendritic cells constitute the major infected cell type during the chronic Leishmania major infection phase of C57BL/6 resistant mice. PLoS Pathog. 2009; 5:e1000494. [PubMed: 19557162]
45. Lim HB, et al. Involvement of superoxide and nitric oxide on airway inflammation and hyperresponsiveness induced by diesel exhaust particles in mice. Free Radic. Biol. Med. 1998; 25:635–644. [PubMed: 9801062]
46. Chang LY, Crapo JD. Inhibition of airway inflammation and hyperreactivity by an antioxidant mimetic. Free Radic. Biol. Med. 2002; 33:379–386. [PubMed: 12126760]
47. Reynaert NL, et al. Catalase overexpression fails to attenuate allergic airways disease in the mouse. J. Immunol. 2007; 178:3814–3821. [PubMed: 17339480]

48. Day RM, Suzuki YJ. Cell proliferation, reactive oxygen and cellular glutathione. Dose Response. 2005; 3:425–442. [PubMed: 18648617]

49. San José G, et al. Insulin-induced NADPH oxidase activation promotes proliferation and matrix metalloproteinase activation in monocytes/macrophages. Free Radic. Biol. Med. 2009; 46:1058–1067. [PubMed: 19439231]

50. Kenyon NJ, Bratt JM, Linderholm AL, Last MS, Last JA. Arginases I and II in lungs of ovalbumin-sensitized mice exposed to ovalbumin: sources and consequences. Toxicol. Appl. Pharmacol. 2008; 230:269–275. [PubMed: 18439639]

51. Umemura N, et al. Tumor-infiltrating myeloid-derived suppressor cells are pleiotropic-inflamed monocytes/macrophages that bear M1- and M2-type characteristics. J. Leukoc. Biol. 2008; 83:1136–1144. [PubMed: 18285406]

52. Sasmono RT, et al. Mouse neutrophilic granulocytes express mRNA encoding the macrophage colony-stimulating factor receptor (CSF-1R) as well as many other macrophage-specific transcripts and can transdifferentiate into macrophages in vitro in response to CSF-1. J. Leukoc. Biol. 2007; 82:111–123. [PubMed: 17438263]

53. Mendoza L, et al. Freezing and thawing of murine bone marrow-derived dendritic cells does not alter their immunophenotype and antigen presentation characteristics. Folia Biol. (Praha). 2002; 48:242–245. [PubMed: 12512800]

54. Hewitt M, Estell K, Davis IC, Schwiebert LM. Repeated bouts of moderate intensity aerobic exercise reduce airway reactivity in a murine asthma model. Am. J. Respir. Cell Mol. Biol. 2010; 42:243–249. [PubMed: 19423772]

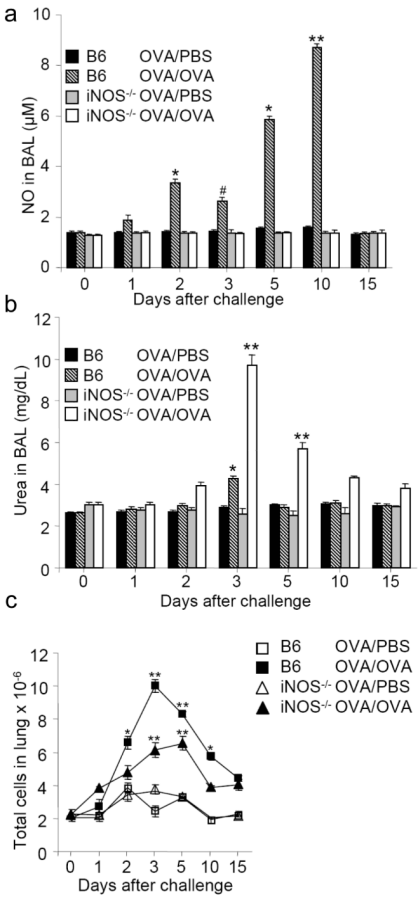

Figure 1.

The iNOS and arginase pathways are induced in a mouse model of allergic airway inflammation.

(a) Measurement using the Griess assay of nitric oxide (NO; measured as the NO metabolite, nitrite) in bronchoalveolar lavage (BAL) fluid harvested at the indicated number of days after challenge. ***P*<0.001 C57BL/6 (B6) mice sensitized and challenged with ovalbumin (OVA/OVA) at d10 vs B6 OVA/OVA mice at d1, d2, d3 & d5, vs control B6 mice sensitized with OVA but mock challenged with PBS (OVA/PBS), and vs inducible nitric oxide synthase-deficient ($iNOS^{-/-}$) OVA/OVA and OVA/PBS mice at all time points. **P*<0.01 B6 OVA/OVA mice at d2 and d5 vs B6 OVA/OVA mice at d1, and vs control B6 OVA/PBS and $iNOS^{-/-}$ OVA/OVA and control OVA/PBS mice. $^{\#}P$<0.05 B6 OVA/OVA mice at d3 vs B6 OVA/OVA mice at d2. **(b)** Measurement of urea in BAL fluid harvested at the indicated number of days after challenge. **P*<0.01 B6 OVA/OVA mice at d3 vs B6 OVA/OVA mice at d2 and d5 and vs control B6 OVA/PBS mice. ***P*<0.001 $iNOS^{-/-}$ OVA/OVA mice at d3 and d5 vs $iNOS^{-/-}$ OVA/OVA mice at d1. **P*<0.01 $iNOS^{-/-}$ OVA/OVA mice at d2 and d10 vs $iNOS^{-/-}$ OVA/OVA mice at d1. ***P*<0.001 for $iNOS^{-/-}$ OVA/OVA mice vs control $iNOS^{-/-}$ OVA/PBS mice. For panels (a) and (b), data are means ± SEM (*n* = 5). (c) Total numbers of infiltrating leukocytes extracted from collagenase digested lung tissue of B6 and $iNOS^{-/-}$ OVA/OVA mice compared to OVA/PBS mice at the indicated times after i.n. challenge. ***P*<0.001 for B6 OVA/OVA mice vs all control OVA/PBS mice and for B6 OVA/OVA mice vs $iNOS^{-/-}$ OVA/OVA mice at d3. ***P*<0.001 for $iNOS^{-/-}$ OVA/OVA mice compared to control $iNOS^{-/-}$ OVA/PBS mice. **P*<0.01 for B6 OVA/OVA

mice vs control OVA/PBS mice and for B6 OVA/OVA mice vs iNOS$^{-/-}$ OVA/OVA mice at d2 and d10. Data are means ± SEM (n = 5).

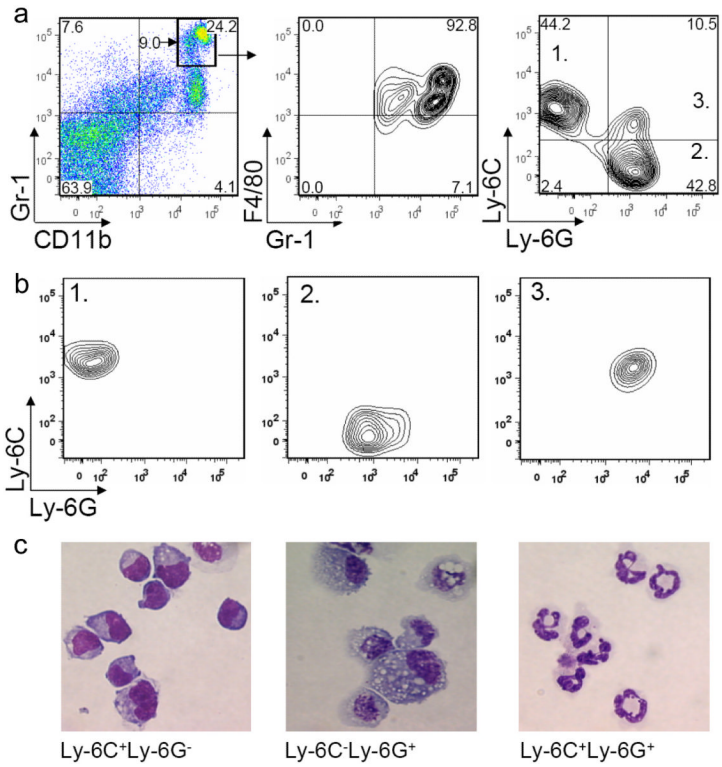

Figure 2.

Distinct myeloid cell subsets with surface phenotypes characteristic of MDSC accumulate in lung tissue during the allergic inflammatory response.

(**a**) Cells recovered from collagenase-digested lung tissue from wt sensitized mice 2d after i.n. OVA challenge and analyzed by FACS demonstrate that the Gr-1^{hi}CD11b^{hi} population is F4/80^{+} (middle panel). The right panel identifies distinct Ly-6C^{+}Ly-6G^{-}, Ly-6C^{+}Ly-6G^{+} and Ly-6C^{-}Ly-6G^{+} subpopulations within the Gr-1^{+}CD11b^{+}F4/80^{+} cells. (b) Flow cytometry profiles of the myeloid cells subsets purified by FACS from the cell preparations analyzed in the right panel of (a). (c) Diff Quick staining of the FACS-purified Ly-6C^{+}Ly-6G^{-}, Ly-6C^{-}Ly-6G^{+} and Ly-6C^{+}Ly-6G^{+} cell populations shown in (b). Magnification × 1000. Similar data were obtained in three additional experiments.

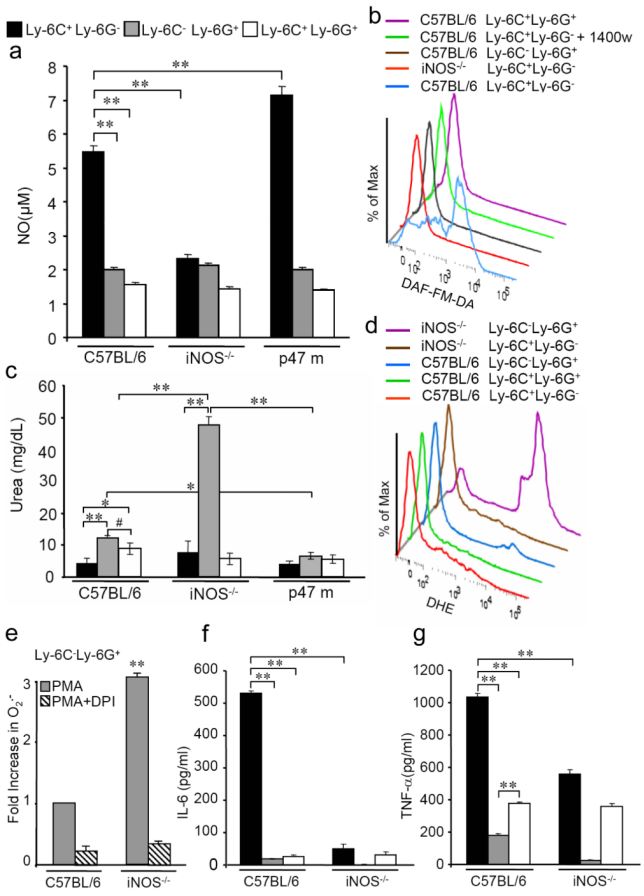

Figure 3.

Distinct free radical and cytokine profiles of lung MDSC-like subsets regulated by the iNOS, NADPH oxidase and arginase pathways.

(**a**) Levels of NO were measured by Griess assay in supernatants of 10^4 FACS purified Ly-6C$^+$Ly-6G$^-$ (black bars) and Ly-6C$^-$Ly-6G$^+$ (grey bars) and Ly-6C$^+$Ly-6G$^+$ (white bars) myeloid cells harvested from lungs of sensitized wt, iNOS$^{-/-}$, or p47m mice (mice with inactive p47 subunit of NADPH oxidase) at d2 after i.n. OVA challenge and cultured for 48h. Data represent means ± SD for triplicate determinations. (**b**) Lung leukocytes recovered on d5 after OVA challenge were stained with DAF-FM-DA, the fluorescent indicator for NO and its metabolites. Positive staining displayed using offset overlaid histograms was detected by FACS analysis of lung Ly-6C$^+$Ly-6G$^-$ cells isolated from wt, but not iNOS$^{-/-}$ mice, and was not detected in Ly-6C$^-$Ly-6G$^+$ or the Ly-6C$^+$Ly-6G$^+$ populations isolated from wt mice. NO production by Ly-6C$^+$Ly-6G$^-$ cells detected by DAF-FM-DA was inhibited when cells were cultured in the presence of 1400w (500 nM). Data represent means ± SD for triplicate determinations. The iNOS$^{-/-}$ mice used to generate the data shown in (b) were studied in the same experiment as the wt mice analyzed in Figures 1 & 4. **(c)** Levels of urea were determined by the DIUR-500 assay using culture supernatants from 10^4 FACS purified Ly-6C$^+$Ly-6G$^-$ (black bars), Ly-6C$^-$Ly-6G$^+$ (grey bars) and Ly-6C$^+$Ly-6G$^+$ (white bars) myeloid cells harvested from lungs of sensitized wt, iNOS$^{-/-}$ mice and p47 m mice at d3 after i.n. OVA challenge. (**d**) Histogram plots of FACS purified Ly-6C$^-$Ly-6G$^+$, Ly-6C$^+$Ly-6G$^-$ and Ly-6C$^+$Ly-6G$^+$ lung myeloid cells, stained with the superoxide-sensitive indicator dye DHE showing positive staining only with Ly-6C$^-$Ly-6G$^+$ cells. Superoxide-producing Ly-6C$^-$Ly-6G$^+$ cells are increased in the iNOS$^{-/-}$ mice. Data shown in (d) are representative of 3 experiments. (**e**) 4 × 10^4 Ly-6C$^-$Ly-6G$^+$ cells, purified

by FACS from the lungs of sensitized and challenged wt and iNOS$^{-/-}$ mice, were activated with PMA in the presence (grey bars) or absence (hatched bars) of DPI. The production of superoxide was determined by spectrophotometric assessment of the kinetics of cytochrome c reduction and expressed as fold increase. Fold increases in cells sorted from iNOS$^{-/-}$ mice were normalized to PMA-stimulated cells from C57BL/6 mice. Data represent means ± SEM (n = 3 mice). **P<0.01 compared to PMA-treated cells from the lungs of wt mice. (**f**) IL-6 and (**g**) TNF-α levels in culture supernatants from Ly-6C^{+}Ly-6G^{-} (black bars), Ly-6C^{-}Ly-6G^{+} (grey bars), and Ly-6C^{+}Ly-6G^{+} (white bars) myeloid cells that had been purified by FACS at d2 after challenge from B6 mice and cultured for 48h were determined by ELISA. For (a) - (g), **P<0.001, *P<0.01 and $^{\#}P$<0.05.

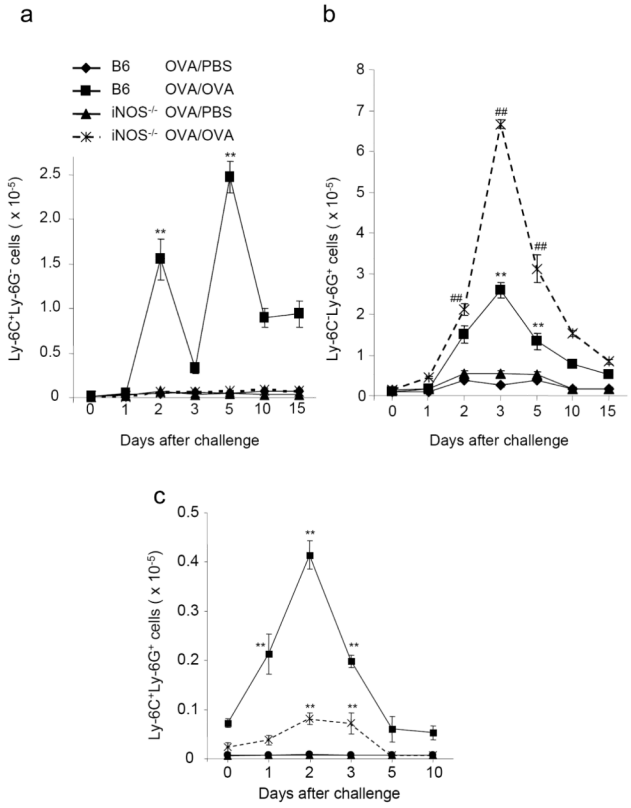

Figure 4.

Differing recruitment dynamics of the MDSC-like subsets during the airway inflammatory response.

The numbers of Ly-6C^{+}Ly-6G^{-} cells (**a**) and Ly-6C^{-}Ly-6G^{+} cells (**b**) recovered as a function of time after OVA challenge of sensitized C57BL/6 (B6) and iNOS$^{-/-}$ mice are compared to control sensitized mice challenged with PBS. (a) $^{**}P<0.001$ comparing the numbers of Ly-6C^{+}Ly-6G^{-} cells in B6 OVA/OVA vs B6 OVA/PBS mice and B6 OVA/OVA vs iNOS$^{-/-}$ OVA/OVA mice. (b) $^{\#\#}P<0.001$ comparing the numbers of Ly-6C^{-}Ly-6G^{+} cells at d2, d3 and d5 after challenge in B6 vs iNOS$^{-/-}$ OVA/OVA mice. $^{**}P<0.001$ comparing the numbers of Ly-6C^{-}Ly-6G^{+} cells at d3 and d5 after challenge in B6 OVA/OVA vs B6 OVA/PBS mice. (**c**) The total numbers of infiltrating Gr-1^{+}CD11b^{+}F4/80^{+}Ly-6C^{+}Ly-6G^{+} granulocyte-like cells in OVA/OVA and OVA/PBS wt and iNOS$^{-/-}$ mice were determined by FACS analysis of collagenase digested lung tissue at the indicated times after challenge. $^{**}P<0.001$ comparing the numbers of Ly-6C^{+}Ly-6G^{+} cells at d1, d2 and d3 after challenge in B6 OVA/OVA vs B6 OVA/PBS mice and in B6 vs iNOS$^{-/-}$ OVA/OVA mice. Data represent means ± SEM ($n = 5$) for all panels.

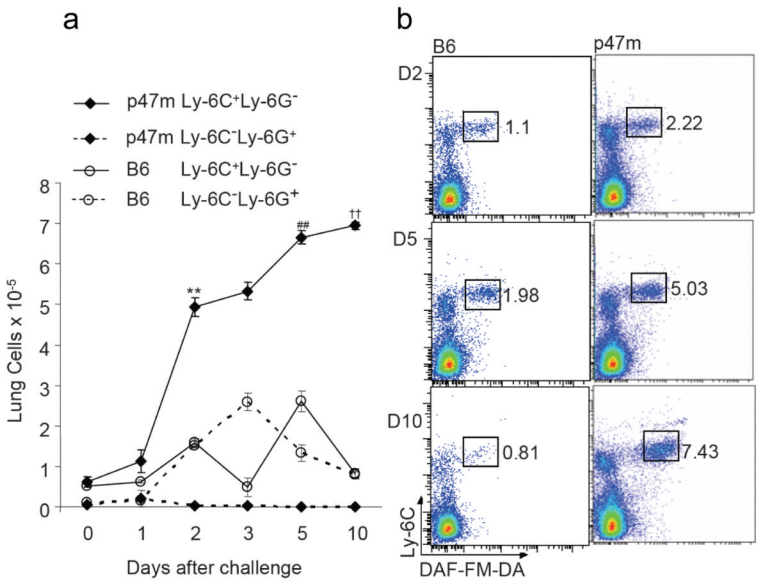

Figure 5.

NADPH oxidase regulates the infiltration of NO-producing myeloid cells during the airway inflammatory response.

(**a**) Total numbers of Ly-6C^{+}Ly-6G^{-} and Ly-6C^{-}Ly-6G^{+} cells recovered from lungs of OVA/OVA B6(Cg)Ncf1m1J/J (p47m) mice and B6 mice harvested at the indicated times after challenge. $^{**}P<0.001$ numbers of Ly-6C^{+}Ly-6G^{-} cells at d2 after challenge; $^{\#\#}P<0.001$ numbers of Ly-6C^{+}Ly-6G^{-} cells at d3 after challenge; and $^{\dagger\dagger}P<0.001$ numbers of Ly-6C^{+}Ly-6G^{-} cells at d5 after challenge, all comparing p47m mice to wt mice. $^{**}P<0.001$ also when comparing the numbers of Ly-6C^{-}Ly-6G^{+} cells vs Ly-6C^{+}Ly-6G^{-} cells in p47m mice. Data represent means ± SEM ($n = 5$). (**b**) Representative FACS plots demonstrating differences in the percentages of cells that are Ly-6C^{+}DAF-FM-DA^{+} in lungs of wt OVA/OVA (left panel) vs p47m OVA/OVA (right panel) mice at d2, d5 and d10 after antigen challenge.

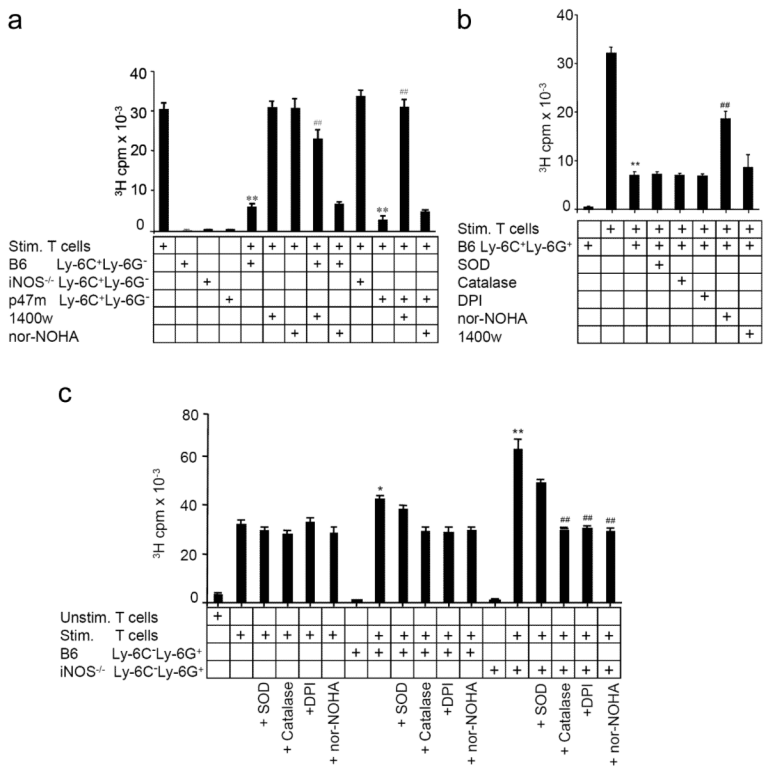

Figure 6.

Subsets of myeloid cells show different abilities to modulate T cell proliferation using the iNOS, arginase and NADPH oxidase pathways.

FACS-purified myeloid cells (10^5 of each subset) from lung tissue of OVA/OVA mice were co-cultured at a 1:1 ratio with naïve B6 CD4$^+$ T cells activated by treatment with anti-CD3 and anti-CD28 antibodies. After 48h, ^{3}H-thymidine was added and incorporated radioactivity was determined 16h later. (**a**) Co-culture of Ly-6C$^+$Ly-6G$^-$ cells from wt, iNOS$^{-/-}$ or p47m mice with naïve T cells in the presence or absence of 1400w or nor-NOHA. $^{**}P<0.001$ compared to stimulated T cells alone; $^{\#\#}P<0.001$ compared to co-culture of wt Ly-6C$^+$Ly-6G$^-$ cells with stimulated T cells. (**b**) Naïve T cells stimulated with anti-CD3 and anti-CD28 antibodies and Ly-6C$^+$Ly-6G$^+$ cells isolated from wt OVA/OVA mice were co-cultured in the presence or absence of the indicated inhibitors. $^{**}P<0.001$ compared to stimulated T cells alone; $^{\#\#}P<0.001$ compared to co-culture of stimulated T cells with Ly-6C$^+$Ly-6G$^+$ cells without inhibitor. (**c**) Ly-6C$^-$Ly-6G$^+$ cells isolated from the lungs of wt or iNOS$^{-/-}$ OVA/OVA mice were cultured with naïve wt T cells and anti-CD3 plus anti-CD28 antibodies in the presence or absence of SOD, catalase, DPI or nor-NOHA. $^{*}P<0.01$ compared to stimulated T cells alone and to co-cultures treated with catalase, DPI or nor-NOHA as indicated; $^{**}P<0.001$ compared to stimulated T cells alone. $^{\#\#}P<0.001$ compared to co-culture of stimulated T cells with Ly-6C$^-$Ly-6G$^+$ cells from iNOS$^{-/-}$ mice. Data are pooled from 4 independent experiments and presented as mean cpm ± SD ($n = 12$).

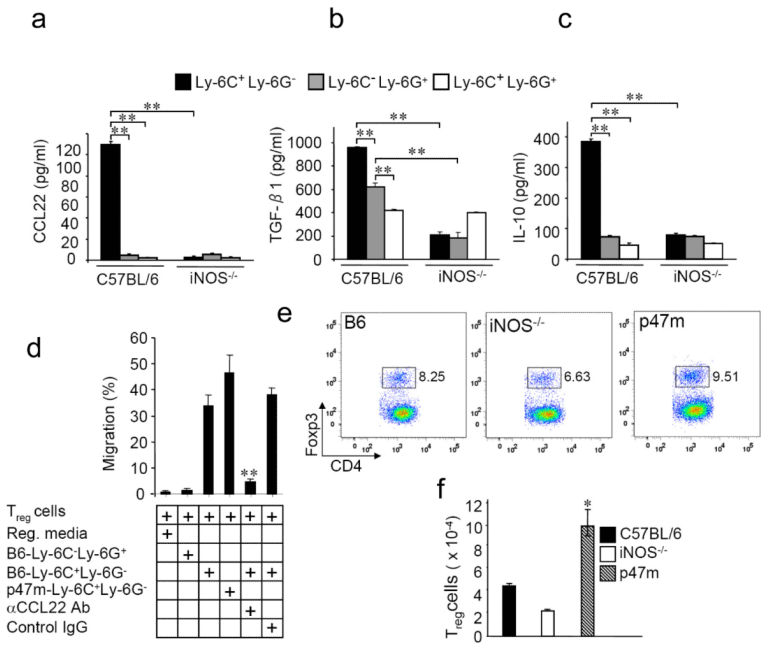

Figure 7.

Ly-6C$^+$Ly-6G$^-$ myeloid cells promote chemotaxis of Foxp3$^+$ T$_{reg}$ cells in a CCL22-dependent manner.

(**a**) CCL22 levels were determined by ELISA using culture supernatants from Ly-6C$^+$Ly-6G$^-$ and Ly-6C$^-$Ly-6G$^+$ myeloid cells sorted from collagenase digests of lung tissue harvested from wt and iNOS$^{-/-}$ OVA/OVA mice at d2 after challenge, then cultured for 24h. Levels of activated TGF-β1 (**b**) and IL-10 (**c**) were determined by ELISA using culture supernatants from sorted Ly-6C$^+$Ly-6G$^-$ (black bars), Ly-6C$^-$Ly-6G$^+$ (grey bars) and Ly-6C$^+$Ly-6G$^+$ (white bars) cells that had been purified from lungs of wt and iNOS$^{-/-}$ OVA/OVA mice at d2 after challenge and cultured for 24h. Data for (a-c) are means ± SD (n = 3 mice). **P<0.001for (a) - (c). (**d**) 10^4 *in vitro* differentiated T$_{reg}$ cells, prepared and purified as described in Materials and Methods, were added to the upper portion of a transwell plate. Supernatants from 48h cultures of purified myeloid cell subsets were added to the lower chambers, with or without anti-CCL22 or control IgG and incubated for 6h. Migrated cells in the lower chambers were quantified by flow cytometric detection of GFP$^+$ cells which express GFP as a fusion protein with the regulatory T cell-specific transcription factor Foxp3. **P<0.001 compared to supernatants of Ly-6C$^+$Ly-6G$^-$ cells from wt mice cultured without added anti-CCL22 or with control IgG. (**e**) Representative FACS plots showing the percent of total infiltrating lung leukocytes that are CD4$^+$Foxp3$^+$(GFP$^+$) at d2 after challenge of wt, iNOS$^{-/-}$ and p47m OVA/OVA mice. (**f**) Total number of CD4$^+$CD25$^+$Foxp3$^+$ T$_{reg}$ cells recovered from collagenase digested lungs d2 after challenge of wt, iNOS$^{-/-}$ and p47m OVA/OVA mice. Data represent means ± SD (n = 3 mice).

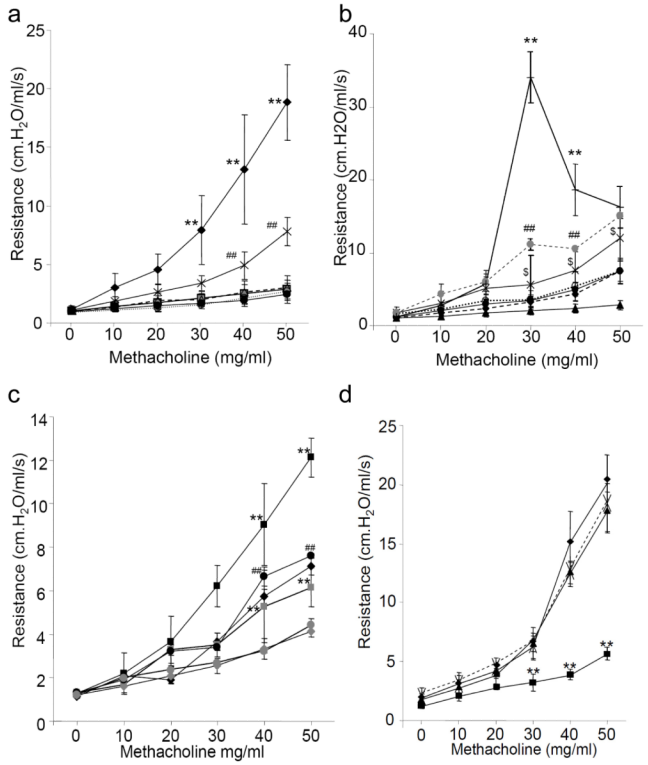

Figure 8.

Intratracheal adoptive transfer of NO- or $O_2^{\cdot -}$-producing myeloid-derived cells modulates airway hyper-responsiveness.

(**a**) Changes in airway resistance (expressed as cm.H2O/ml/s) following methacholine challenge of sensitized iNOS$^{-/-}$ (◆), p47m (△), and wt (✳) mice that had received OVA challenge 3d previously or sensitized iNOS$^{-/-}$ (□), p47m (●), or wt (⊙) mice that received PBS challenge 3d previously. $^{**}P$<0.001 (◆) vs (✳); $^{\#\#}P$<0.001(✳) vs (△). (b) Modulation of airway resistance in OVA/OVA wt (◆) recipient mice following adoptive transfer of PBS (●), or 10^5 Ly-6C$^+$Ly-6G$^-$ (▲) or Ly-6C$^-$Ly6G$^+$ (●) cells sorted from OVA/OVA wt mice, 10^5 Ly-6C$^+$Ly-6G$^-$ (✕) and Ly-6C$^-$Ly6G$^+$ (|) cells sorted from OVA/OVA iNOS$^{-/-}$ mice, or 10^5 sorted wt BMDC (⊙). ** and $^{\#\#}P$<0.001 comparing (|) and (●) to (●), and (|) and (●) to (▲), respectively; $^{\$}P$<0.01 comparing (✳) to (●). (c) Modulation of airway resistance in OVA/OVA wt (●) (n=3 mice) or p47m (●) (n= 3 mice) following control mock adoptive transfer with PBS, or in OVA/OVA recipient wt mice following adoptive transfer with 10^5 Ly-6C$^-$Ly-6G$^+$ lung cells sorted from OVA/OVA wt mice (■) (n=10 mice) or 10^5 wt Ly-6C$^-$Ly-6G$^+$ lung cells sorted and treated with DPI (◆) (n=12 mice), OVA/OVA recipient p47m mice following adoptive transfer with 10^5 Ly-6C$^-$Ly-6G$^+$ lung cells sorted from OVA/OVA wt mice (□) (n=6 mice) or 10^5 wt Ly-6C$^-$Ly-6G$^+$ lung cells sorted and treated with DPI (◇) (n=11 mice). $^{**}P$<0.001 comparing (◆) to (■) and comparing (□) to (◇). $^{\#\#}P$<0.001 comparing (●) to (●). (d) Changes in airway resistance in OVA/OVA iNOS$^{-/-}$ mice (▲) following adoptive transfer of PBS (✳), 10^5 Ly-6C$^+$Ly-6G$^-$ cells sorted from OVA/OVA wt mice (■) or 10^5 purified, *in vitro* differentiated wt BMDC (◆). $^{**}P$<0.001 comparing to (✳). Data are means ± SD, n = 8-11 for (a) and (b), n = 6 for (c).

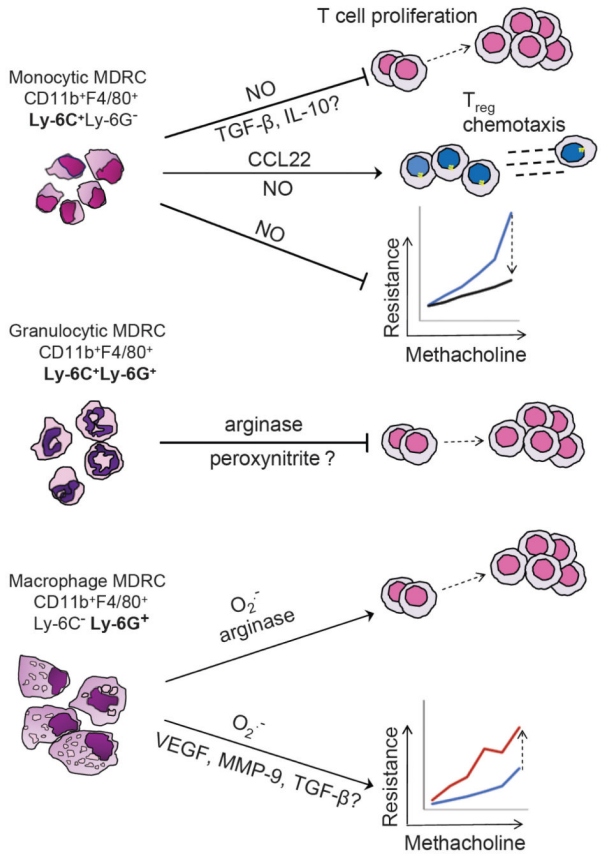

Figure 9.

Free radical-producing MDRC are master regulators of airway inflammation.

The three subsets of the myeloid lineage cells defined here express and use metabolites of the free radical pathways to differentially regulate T cell proliferation, T_{reg} cell chemotaxis and AHR. The monocytic and granulocytic MDRC provide generally anti-inflammatory signals that suppress $CD4^+$ T cell proliferation and AHR, whereas the macrophage-like MDRC enhance $CD4^+$ T cell proliferation and exacerbate AHR. NO produced by the iNOS pathway or its metabolites regulate the numbers of Ly-$6C^-$Ly-$6G^+$ $O_2^{\cdot -}$-producing cells that are recruited to the lungs, whereas NADPH oxidase-derived $O_2^{\cdot -}$ regulates the numbers of recruited Ly-$6C^+$Ly-$6G^-$ NO-producing cells. The relative balance between pro- and anti-inflammatory MDRC contributes importantly to setting the inflammatory rheostat in the lungs.